

Photocatalytic properties of TiO_2 bonded active carbon composites prepared by SOL-GEL^①

LI You-ji(李佑稷)^{1, 2}, LI Xiao-dong(李效东)², LI Jun-wen(李君文)³, YIN Jing(尹静)³

(1. College of Chemistry and Chemical Engineering, Jishou University, Jishou 416000, China;

2. State Key Laboratory of New Ceramic Fibers and Composites,

School of Aerospace and Materials Engineering,

National University of Defence Technology, Changsha 410073, China;

3. Institute of Hygiene and Environmental Medicine,

Academy of Military Medical Science, Tianjin 300050, China)

Abstract: Photocatalyst of TiO_2 bonded active carbon (TiO_2/AC), was prepared via sol-gel method from a mixture of TiO_2 sol with active carbon. Post heat treatment was performed at 250 °C for 2 h in air and then kept at 400 °C to 600 °C under a flow of nitrogen for 2 h. The TiO_2/AC composites obtained were characterized by SEM, XRD, UV-vis and BET. The photocatalytic activities of the TiO_2/AC composites were studied in comparison with TiO_2 , AC, P-25 and a mixture of TiO_2 and AC, respectively. The Ramnant rate of Rhodamine B absorbed by the active carbon is found to be almost 70% and the remnant rates of the Rhodamine B decolorized by TiO_2 and the mixture of TiO_2 and the active carbon are 30% and 25%, respectively. However, nearly complete removal of Rhodamine B is observed for a TiO_2/AC composite after 200 min under UV irradiation, which will take the P-25 commercial product 5 h. Therefore, the TiO_2/AC composite is much more effective in decolorization of aqueous Rhodamine B. In addition, the composite can be easily separated from solutions.

Key words: TiO_2 -bonded composite; sol-gel; photoactivity; active carbon

CLC number: TQ 134

Document code: A

1 INTRODUCTION

Environmental purification using photocatalysts has attracted a great deal of attention due to the increasing environmental problems in the world^[1]. Recently, their application has been focused on the purification and treatment of water and air^[2]. TiO_2 is the a promising and wildly used photocatalyst because of its high activity, chemical stability, robustness against photocorrosion, low toxicity, nor-twain pollution and availability at low cost^[3-5]. However, shortcomings of conventional powder catalysts are owing to the low efficiency in making use of light, difficulty in stirring during reaction and separation after reaction and low-concentration contamination near TiO_2 ^[6, 7]. These disadvantages of TiO_2 result in low efficiency in photocatalytic activity in practical application. Correspondingly, catalysts such as TiO_2 bonded active carbon(TiO_2/AC) were prepared to overcome these disadvantages and to extend its industrial applications. It is efficient to shelter low-concentration contamination that the higher BET surface area of active carbon act as the carrier of TiO_2 powder^[8]. Some papers reported on preparation of the composites between TiO_2 and carbon^[9-12] and TiO_2

mounted exfoliated graphite^[13, 14]. It was reported that the addition of active carbon to titania slurry could increase decomposition of some organic compounds during the photocatalytic process^[15]. In other group's work, mounting of TiO_2 onto various active carbons was reported to result in certain reduction of specific surface area of carbons and TiO_2 broke away from active carbon^[12]. This was reasonably supposed to be owing to the preferential deposition of TiO_2 particles at the entrance of the miniature pores of active carbon and TiO_2 particles felted on the surface of active carbon by fixed glue. In the present work, the sol-gel technique is applied in order to introduce TiO_2 into the inside and outside of active carbon and increase their binding energy, aiming to avoid precipitation of TiO_2 into miniature pores of active carbon by adjusting the ratio of active carbon to TiO_2 sol and restrict TiO_2 desquamating from active carbon by heat treatment. In this work, composites of TiO_2/AC with high photocatalytic activity are successfully prepared and their photocatalytic properties are studied.

2 EXPERIMENTAL

2.1 TiO_2/AC composites preparation

① **Foundation item:** Project supported by the National Defence of Academy of Military Medical Science

Received date: 2004-03-16; **Accepted date:** 2004-09-06

Correspondence: LI You-ji, PhD Candidate; Tel: + 86-13787118865; Fax: + 86-731-4573166; E-mail: bcclyj@163.com

Precursor solutions for TiO_2/AC were prepared by the method^[3] as follows. Tetrabutylorthotitanate (Aldrich, 99.9%, 17.02 mL) and diethanolamine (4.8 mL) were dissolved in ethanol (64.82 mL). The solution was stirred vigorously for 2 h at 20 °C followed by addition of a mixture of distilled water (0.9 mL) and ethanol (10 mL) on stirring. The resulted alkoxide solution was left standing at 20 °C for 2 h for hydrolysis reaction, resulting in the TiO_2 sol. The chemical composition of the starting alkoxide solution was $x[\text{Ti}(\text{OC}_4\text{H}_9)_4]:x(\text{C}_2\text{H}_5\text{OH}):x(\text{H}_2\text{O}):x[\text{NH}_2(\text{C}_2\text{H}_4\text{OH})_2] = 1:25.5:1:1$. Then a desired amount of active carbon particles (AC) (pure chemicals) was used as the carriers and was added into TiO_2 sol. After this sol changed to gel, TiO_2 gel bonded active carbon was heat treated at 250 °C for 2 h in air and then heating temperature was increased gradually to the end temperature from 400 °C to 600 °C for 2 h in nitrogen using an electric oven. The concentration of TiO_2 sol in active carbon was adjusted by the quantity of active carbon added to TiO_2 sol.

2.2 Photocatalytic activity evaluation

Photocatalytic activity of the TiO_2/AC was determined by aqueous Rhodamine B decolorization in water under UV irradiation. The same mass (0.5 g) of TiO_2/AC , AC, TiO_2 and mixture of TiO_2 with AC (the amount of TiO_2 in mixture is equal to that of TiO_2 in TiO_2/AC) were added respectively into aqueous Rhodamine B with a concentration of 5 mmol/L in a quartz cell (280 mL), as presented in Fig. 1. An ultraviolet lamp of 40 W, fixed in the middle of the quartz cell, was used as a light source, with wavelength range and peak wavelength of 320–400 nm and 365 nm, respec-

tively. The solution was sparged with air during irradiation. The concentration of Rhodamine B after decolorization was determined by an UV-visible spectrophotometer. The photocatalytic decolorization of Rhodamine B is a pseudo-first-order reaction and its kinetics may be expressed as $\ln\left(\frac{C_0}{C}\right) = k_{\text{app}}C$.

2.3 Characterization

The crystallinity of the TiO_2/AC was determined by X-ray diffraction (XRD) using an HZG4-PC diffractometer with $\text{Cu K}\alpha$ radiation, the accelerating voltage and the applied current were 35 kV and 20 mA, respectively. The crystalline size of TiO_2/AC and TiO_2 was calculated from XRD measurement by supplied computer program. The concentration of anatase was estimated from integrated intensities of the reflection of (101) and (110) phases. The amount of TiO_2 bonded on the carbon surface was determined from ignition loss at 700 °C in air by using TG apparatus (STA 449 C Jupiter 8 thermobalance of Netzsch Company, Germany). The structure of prepared catalysts was observed on using scanning electron microscope (SEM, SX-100) with an accelerating voltage of 20 kV. The size of TiO_2 grains in TiO_2/AC composites and TiO_2 was observed using an UV-visible spectrophotometer (Helios of Unicam company, England) with a wavelength range of 200–1 000 nm. BET surface area was determined with a monosorb BET analyzer (Quantachrome Company, USA).

3 RESULTS AND DISCUSSION

3.1 Photocatalytic activity of TiO_2/AC

The results of Rhodamine B removal under UV irradiation are presented in Fig. 2. The remnant rate of Rhodamine B, decolorized by active carbon under UV irradiation without photocatalysis, was found to be 70% after 200 min. The remnant rate of the Rhodamine B decolorized by the TiO_2 and UV irradiation are 30% and 96% after 200 min, respectively. However, heated to an end temperature of 500 °C for 2 h, the TiO_2/AC containing both anatase and rutile phase reaches almost 100% of the Rhodamine B removal. This seems to suggest that the effect of the active carbon carriers must appear remarkably. To demonstrate further the utility of the active carbon carriers for TiO_2 loading, photodecomposition of Rhodamine B was studied using the naked TiO_2 in the presence of dispersed active carbon. As shown in Fig. 2, the reaction rate of the naked TiO_2 was increased by introducing the active carbon into the TiO_2 suspension. The remnant rate of the Rhodamine B decolorized by the mixture of TiO_2 with active carbon was 25%, but the enhancement was not so great as that obtained at the 26.3%-loaded TiO_2/AC . It may attribute

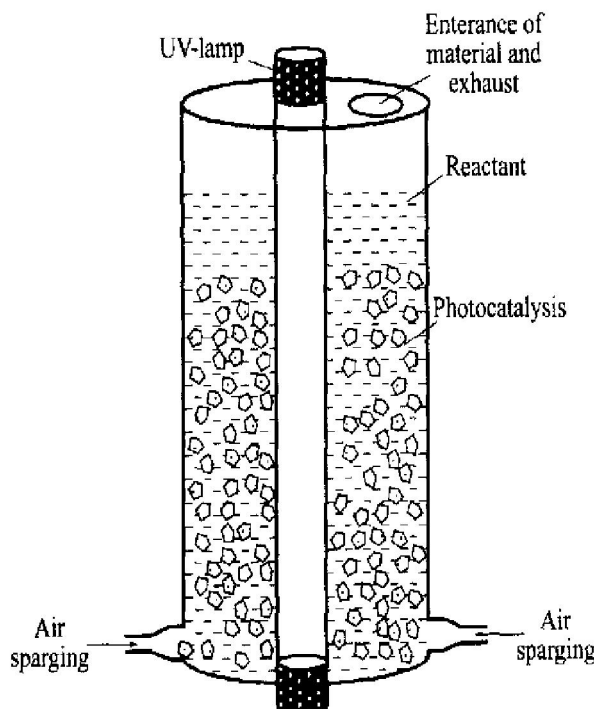


Fig. 1 Setup of photocatalytic reaction

this to the active carbon with high surface area, which worked well as an effective adsorbate to concentrate Rhodamine B around the loaded TiO_2 . The adsorbed Rhodamine B seems to be supplied to the loaded TiO_2 mostly by surface diffusion. In addition, active carbon can possibly prevent recombination of electron-hole pairs. The presence of Ti^{3+} ion, which could capture generated electrons, is confirmed by XPS survey spectra under effect of active carbon. UV irradiation was essential to photodegradation of Rhodamine B by TiO_2/AC , because the remnant rate of the Rhodamine B decolorized by the TiO_2/AC without UV is 68%.

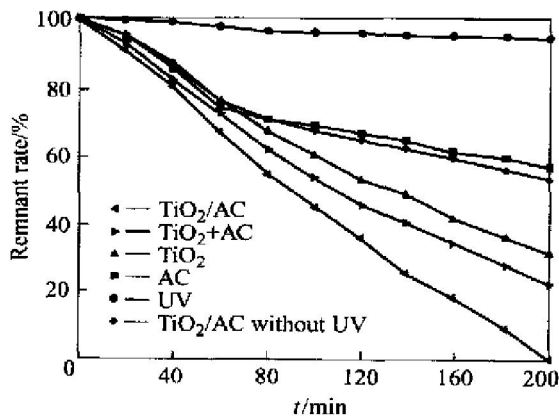


Fig. 2 Photocatalytic degradation properties of TiO_2/AC , TiO_2 , AC and mixture of TiO_2 powder with AC, pyrolyzed under same condition at 500 °C

The photoactivity was compared to commercially available TiO_2 P-25 (Degussa, Germany) that consists of both anatase (80%) and rutile (20%) phases of TiO_2 . The same experimental conditions were selected for P-25. From the comparison between catalysts P-25 and the TiO_2/AC composite (in Fig. 3.), it can be seen that Rhodamine B undergoes decomposition much faster in the case of the latter catalyst. After 200 min of irradiation at

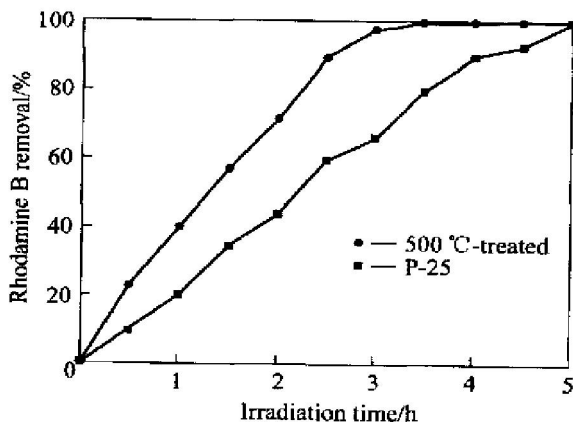


Fig. 3 Rhadamine B removal under UV irradiation with P-25 and 500 °C-treated catalysts

most 100% Rhodamine B removal was observed, but the former needed at least 5 h.

IR spectra of Rhodamine B show that some organic compounds emerged after it was photodegraded, as illustrated in Fig. 4. The new bands in the range of 1 150 – 1 270 cm^{-1} are attributed to $\text{C}=\text{O}$ vibration of carbonate or ether species. The apparent reaction rate constants of the photocatalytic decolorization of Rhodamine B was 0.007 min^{-1} for TiO_2/AC and 0.005 0 min^{-1} for TiO_2 , respectively.

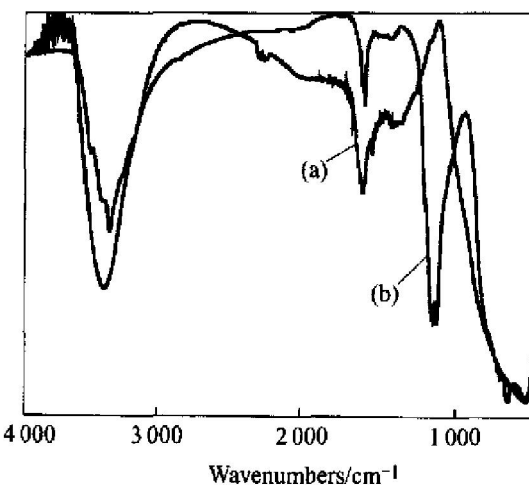


Fig. 4 IR spectra of Rhodamine B before (a) and after (b) decolorization

3.2 XRD results

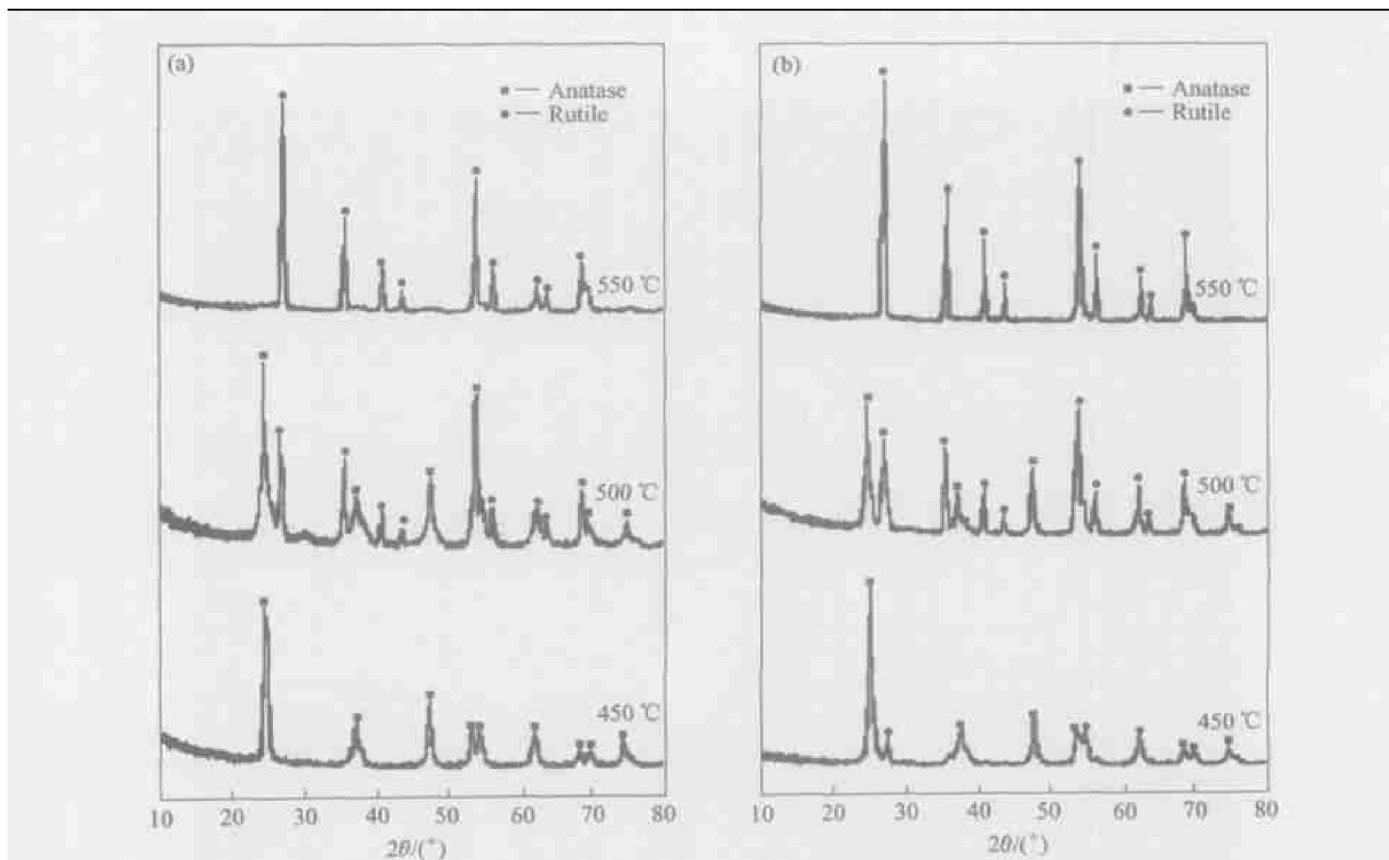
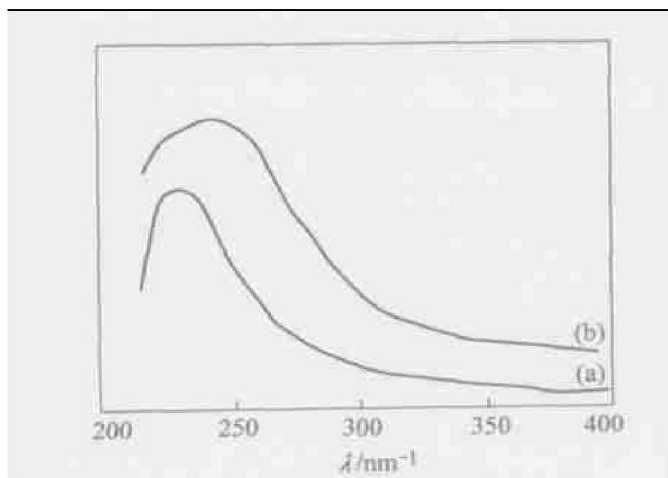
XRD patterns of TiO_2/AC and TiO_2 under different heat-treated temperatures are presented in Fig. 5 and Table 1. The TiO_2/AC heated to 450 °C for 2 h consists only of anatase phase of TiO_2 , while that heated at 500 °C consists of both anatase (65%) and rutile (35%). Crystalline phase of anatase was developed in TiO_2/AC with the increase of heat-treatment temperature. The higher the heat-treatment temperature, the larger the amount of rutile formed. When the heat-treatment temperature was 550 °C for 2 h, TiO_2/AC consists of only rutile. However, the TiO_2 consists of both anatase (95%) and rutile (5%) phases at heat-treatment temperature of 450 °C for 2 h. When the TiO_2 was heated from 500 °C to 550 °C, the content of anatase of TiO_2 varied from 45% to 0. The crystallite size of TiO_2/AC and TiO_2 were rising with the increasing heat-treatment temperature. At the same heat-treatment temperature, the crystallite size of TiO_2 was greater than that of TiO_2/AC and the increasing degree of the grain size of TiO_2 is faster than that of TiO_2/AC . This may be attributed to the fact that the active carbon has such a great surface area that it retards the growth of TiO_2 crystallite bonded active carbon.

3.3 UV-vis spectra

Fig. 6 shows the UV-vis spectra in the wave-

Table 1 Anatase content and crystalline grain size of TiO_2/AC and TiO_2 under different heat-treatment conditions for 2 h

Temperature/ °C	Mass fraction of anatase/ %		Crystalline grain size/ nm	
	TiO_2/AC	TiO_2	TiO_2/AC	TiO_2
450	100	95	26.8	34.7
475	88	71	30.2	40.3
500	65	45	37.5	47.2
525	32	25	39.1	49.8
550	0	0	42.7	53.3

**Fig. 5** XRD patterns of TiO_2/AC composites (a) and TiO_2 nanor-powders (b) pyrolyzed at different temperatures**Fig. 6** UV-vis absorption spectra of TiO_2/AC (a) and TiO_2 (b)

length range 200 – 400 nm for TiO_2 grains in composites

and TiO_2 grains, respectively. The absorption edge of the TiO_2/AC (Fig. 6(a)) is observed at a lower wavelength range than that of the TiO_2 (Fig. 6(b)). The shift is ascribed to the difference in particle size. The TiO_2/AC composites contain relatively small particle and show a pseudo "blue shift". This is adapt to the obtained results by XRD. The BET surface areas of TiO_2/AC , TiO_2 and active carbon are presented in Table 2. The BET surface area of the active carbon in TiO_2/AC rises slightly with the increasing heat-treatment temperature. At the same time, the BET surface area of TiO_2 reduces as the grain size of TiO_2 raised. It causes development of surface area of TiO_2/AC that the big carves in active carbon changes into small carves with the decreasing mass of TiO_2/AC .

3.4 SEM results

Fig. 7 shows the scanning electron micrograph of the surface of TiO_2/AC and TiO_2 . It is observed

Table 2 BET surface area of TiO_2/AC and TiO_2 under different heat-treatment conditions

Heat-treatment temperature/ °C	$w(\text{TiO}_2)/\%$	BET surface area/ ($\text{m}^2 \cdot \text{g}^{-1}$)		
		TiO_2/AC	TiO_2	AC
450	17.8	510.97	76.13	434.8
475	21.6	519.86	74.31	436.3
500	26.3	526.03	70.71	440.1
525	30.2	538.78	68.65	444.8
550	34.1	556.94	66.44	447.1

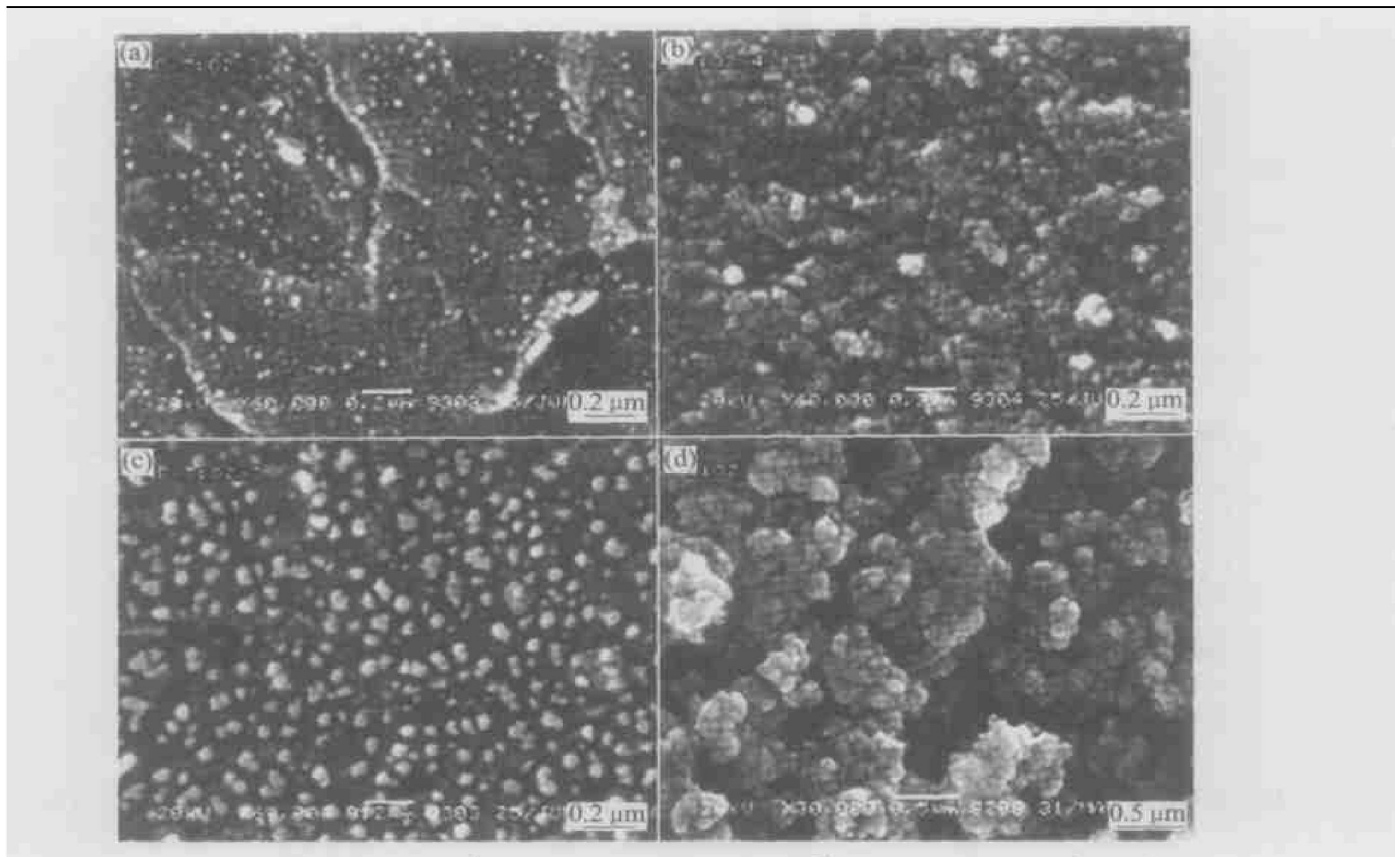


Fig. 7 SEM images after heat-treated under different conditions for 4 h
 (a) $-\text{TiO}_2/\text{AC}$ at 400 °C; (b) $-\text{TiO}_2$ at 400 °C; (c) $-\text{TiO}_2/\text{AC}$ at 500 °C; (d) $-\text{TiO}_2$ at 500 °C

that the TiO_2/AC has spherical microstructure and dispersing texture, composed of 30~50 nm sphere particles. However, the grain size of TiO_2 with reuniting microstructure is bigger than that of TiO_2/AC . In accordance with the increasing heat-treatment temperature, the grain sizes of TiO_2/AC and TiO_2 increase, but the increasing degree of the grain size of TiO_2 is faster than that of the grain size of TiO_2/AC . This is due to the great surface area of the active carbon that has a great “absorbing energy” to retard growth of TiO_2 grains.

4 CONCLUSIONS

In order to prepare TiO_2 bonded active carbon composite with higher photoactivity, the active carbon was

added into TiO_2 sol by properly controlling the ratio of active carbon to TiO_2 sol. Introducing active carbon into the TiO_2 composite would not decrease its surface area, instead, some advantages can be obtained, such as suppression of anatase onto rutile phase and retarding growth of TiO_2 grains. The prepared catalysts can effectively remove rhodamine B under UV irradiation and can be easily separated from solutions, which is due to the active carbon carrier.

REFERENCES

- [1] Kawasaki K, Despres J F, Kamei S, et al. Photocatalytic oxidation of organics in water using pure and silver-modified titanium dioxide particles [J]. Journal of Photochemistry and

Photobiology A: Chemistry, 2002, 148: 233 – 245.

[2] Gao W, Wu F Q, Luo Z, et al. Studies on the relationship between the crystal form of TiO₂ and its photocatalyzing degradation efficiency [J]. Chem J Chinese Universities, 2001, 22: 660.

[3] Znaldi L, Seraphimova R, Bocquet J F, et al. A semi-continuous process for the synthesis of nanosize TiO₂ powder and their use as photocatalysts [J]. Mat Res Bull, 2001, 36: 812.

[4] Hoffman M R, Martin S T, Choi W. Environmental application of semiconductor photocatalysis [J]. Chem Rev, 1995, 95: 69 – 96.

[5] Vicente G S, Morales A, Gutierrez M T. Preparation and characterization of sol-gel TiO₂ antireflective coatings for silicon [J]. Thin Solid Films, 2001, 391: 133 – 137.

[6] Herrmann J M, Guillard C, Disdier J, et al. New industrial titania photocatalysts for the solar detoxification of water containing various pollutants [J]. Applied Catalysis B: Environmental, 2002, 35: 281 – 294.

[7] Takeda N, Torimoto T, Sampath S, et al. Effect of inert supports for titanium dioxide loading on enhancement of photodecomposition rate of gaseous propionaldehyde [J]. J Phys Chem, 1995, 99: 9986 – 9991.

[8] Uchida H, Itoh S, Yoneyama H. Photocatalytic decomposition of propyzamide using TiO₂ supported on activated carbon [J]. Chem Lett, 1993, 22: 1995 – 1998.

[9] El-Sheikh A H, Newman A P, Al-Daffaee H, et al. deposition of anatase on the surface of activated carbon [J]. Surface and Coatings Technology, 2004, 187: 284 – 292.

[10] Lettmann C, Hildenbrand K, Kisch H, et al. Visible light photodegradation of 4-chlorophenol with a coke-containing titanium dioxide photocatalyst [J]. Appl Catal B, 2001, 32: 215 – 227.

[11] Zhang F S, Nriagu J O, Itoh H. Photocatalytic removal and recovery of mercury from water using TiO₂-modified sewage sludge carbon [J]. Journal of Photochemistry and Photobiology A: Chemistry, 2004, 167: 223 – 228.

[12] Tryba B, Morawski A W, Inagaki M. A new route for preparation of TiO₂-mounted activated carbon [J]. Appl Catal B, 2003, 41: 427.

[13] Tsumura T, Kojitani N, Umemura H, et al. Composites between photoactive anatase-type TiO₂ and adsorptive carbon [J]. Appl Surf Sci, 2002, 196: 429 – 436.

[14] Modestov A. D, Lev O. Photocatalytic oxidation of 2, 4-dichlorophenoxyacetic acid with titania photocatalyst. Comparison of supported and suspended TiO₂ [J]. J Photochem Photobiol A, 1998, 112: 261 – 270.

[15] Silva C G, Faria J L. Photochemical and photocatalytic degradation of an azo dye in aqueous solution by UV irradiation [J]. Journal of Photochemistry and Photobiology A: Chemistry, 2003, 155: 133 – 143.

(Edited by LONG Huai-zhong)